

Research Article

The Parameters Optimization of Water Jet Processing Nozzles' Internal Flow Field Applied in Scallops Shucking Device

¹Jiazhong Wang, ²Guihong Zhou and ¹Qiushi Li

¹College of Mechanical and Electrical Engineering,

²College of Information Science and Technology, Agriculture University of Hebei, Baoding 071001, P.R. China

Abstract: In order to seek for the effective, inexpensive and safer methods and technologies to shuck the adductor muscle from Scallop in Shell, the water jet technology is introduced and its experimental study was carried out. The nozzle is critical component in shucking device and nozzle parameters, such as cone angle ϕ , outlet diameter d and outlet length S , would affect the flow velocity distribution. In order to determine the influence of nozzle parameters and optimize the nozzle structure, the simulation analyses for scallop stripping equipment nozzle internal flow field are conducted. The narrow-angle fan nozzle's internal flow field was simulated using standard $k-\varepsilon$ turbulence model with CFX software. After comprehensive analysis, the optimal parameters combinations of the nozzle for water jet processing were obtained. The result of this research has very important application value for the design and optimization of scallops shelling device.

Keywords: Internal flow field, parameter optimization, scallop shucking processing, simulation analysis, water jet

INTRODUCTION

Scallop adductor muscle is not only of high nutritional value, but it also has a high value of medicinal (Cuili and Sai, 2001; Lunn and Theobald, 2006; Li *et al.*, 2011). Shucking scallops involves not only separating the shells of the scallop but also severing or causing a release of the adductor muscle from these valves (Namba *et al.*, 1995). It is a difficult problem to shuck the adductor muscle from Scallop in Shell in the research field of seafood processing. Over one hundred patents and innovations in areas, Scallop shucking method is generally divided into mechanical and non-mechanical method (Martin and Hall, 2006; He *et al.*, 2002; Cooper, 2010; Qiushi, 2014; Li *et al.*, 2013; Cruz-Romero *et al.*, 2004; Martin, 2004; Dunn *et al.*, 2000; Xie, 2015). Mechanical peeling method generally includes two stages: using a special mechanical device to open the shell and the adductor muscle being stripped by force from the shell. Non-mechanical method generally includes thermal shock method, negative pressure adsorption, water bath method and ultra high pressure method. However, due to its special physiological structure, the ideal shell shucking method has not been found yet. It is a critical job for us to seek for advance technologies that are

effective, inexpensive and safer than previously available technologies.

Water jet cutter technology is based on the naturally erosive effects of water. A stream of water is extremely concentrated and shot out of a nozzle at 30,000-90,000 psi. Water jet cutters work on the same principle as high pressure washers that essentially "cut" the dirt off of the surfaces on which they are used. Cutters have the stream of water greatly intensified and are able to cut through materials both safely and accurately (Qiushi, 2014; Hreha *et al.*, 2010; Xie, 2015). Water jet technology is both a safe and green technology. In recent years, water jet is applied to all kinds of industries and it has been widely used in food and medical fields (Papachristou and Barters, 1982; Qiushi, 2014; Dunn *et al.*, 2000; Hreha *et al.*, 2010; Yoshiaki, 2006; Xie, 2015). The another advantage of this technology is that It's has the lack of thermal effect on machined material. However, possibilities of its further usage have not been exhausted yet. Scallop shucking processing is a field where this technology is used little.

The water jet technology is introduced into the Bay of Scallop in Shell adductor muscle shucking and its experimental study was carried out. The type of jet shucking adductor muscle is determined as non

Corresponding Author: Jiazhong Wang, College of Mechanical and Electrical Engineering, Agriculture University of Hebei, Baoding 071001, P.R. China

This work is licensed under a Creative Commons Attribution 4.0 International License (URL: <http://creativecommons.org/licenses/by/4.0/>).

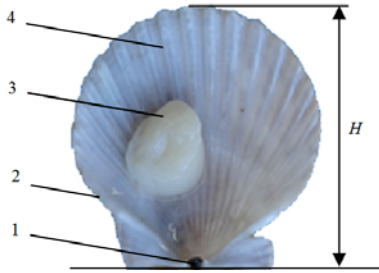


Fig. 1: The Structure and geometric parameters of scallops; 1. Hinge, 2. Shell, 3. adductor muscle, 4. Radial rib

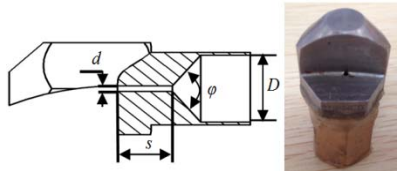


Fig. 2: The physical structure of narrow-fan- nozzle

submerged water jet by comparative analysis. The nozzle is one of the key components of the stripping device. The results of test reveal that it is ideal to use narrow angle fan-shaped nozzle stripping adductor muscle. The purpose of the precise separation of the scallop from the shell is achieved. The research target is internal flow field state and the outlet velocity distribution of the water jet injection.

MATERIALS AND METHODS

Preparation of bay scallop sample: Take the fresh bay scallop ($H = 55\sim 60$ mm) as the test sample, which the shell, skirts, visceral have been removed (only retained under shell and adductor muscle). Figure 1 is the structure and geometric parameters of scallops.

The mathematical model of wather jet:

Nozzle physical model: Figure 2 is the physical model of the internal structure of the narrow angle sector nozzle. The assumption is that the narrow angle sector nozzle internal media is pure water which is incompressible. The water flow from the main nozzle and eject from the narrow end, through the contraction. In this study, the liquid flow in the nozzle is regard as turbulent flow.

The main parameters of nozzles are entrance diameter D , nozzle outlet diameter d , outlet length s and outlet nozzle cone angle ϕ . Where s , d and ϕ are the dominant parameters, by which the nozzle entrance diameter D can be defined. So the influence of ϕ , s and d on nozzle outlet velocity is the main emphasis content in this study.

The mathematical model of water jet: Suppose the flow in water jet is a free jet. To approximate the real fluid as an ideal fluid, the mathematical description of

the ideal fluid mechanics equation is established. In Cartesian coordinate system, the equation of kinematics of ideal fluid is as follows (Currie, 2012):

$$\frac{\partial \rho}{\partial t} + \frac{\partial \rho u}{\partial x} + \frac{\partial \rho v}{\partial y} + \frac{\partial \rho w}{\partial z} = 0 \quad (1)$$

$$\frac{\partial u}{\partial t} + u \frac{\partial u}{\partial x} + v \frac{\partial u}{\partial y} + w \frac{\partial u}{\partial z} = -\frac{1}{\rho} \frac{\partial p}{\partial x} + f_x \quad (2)$$

$$\frac{\partial v}{\partial t} + u \frac{\partial v}{\partial x} + v \frac{\partial v}{\partial y} + w \frac{\partial v}{\partial z} = -\frac{1}{\rho} \frac{\partial p}{\partial y} + f_y \quad (3)$$

$$\frac{\partial w}{\partial t} + u \frac{\partial w}{\partial x} + v \frac{\partial w}{\partial y} + w \frac{\partial w}{\partial z} = -\frac{1}{\rho} \frac{\partial p}{\partial z} + f_z \quad (4)$$

Assuming that the water jet flow is in a fully turbulent state, the standard $k-\varepsilon$ equation model is chosen and the turbulent kinetic energy K and dissipation rate ε equations of the standard equation model are as follows:

k equation:

$$\frac{\partial(\rho k)}{\partial t} + \frac{\partial(\rho k u_i)}{\partial x_i} = \frac{\partial}{\partial x_j} \left[\left(\mu + \frac{\mu_t}{\sigma_k} \right) \frac{\partial k}{\partial x_j} \right] + G_k + G_b - \rho \varepsilon - Y_M + S_k \quad (5)$$

ε equation:

$$\frac{\partial(\rho \varepsilon)}{\partial t} + \frac{\partial(\rho \varepsilon u_i)}{\partial x_i} = \frac{\partial}{\partial x_j} \left[\left(\mu + \frac{\mu_t}{\sigma_\varepsilon} \right) \frac{\partial \varepsilon}{\partial x_j} \right] + C_{1\varepsilon} \frac{\varepsilon}{k} (G_k + C_{3\varepsilon} G_b) - C_{2\varepsilon} \rho \frac{\varepsilon^2}{k} + S_\varepsilon \quad (6)$$

where,

G_k = Turbulent kinetic energy due to the mean velocity gradient

G_b = Turbulent kinetic energy induced by buoyancy

$C_{1\varepsilon}$, $C_{2\varepsilon}$ are constants, the value is 1.44, 1.92 respectively; $C_{3\varepsilon} = 0$, the main direction is perpendicular to the direction of gravity; $\sigma_k = 1.0$, $\sigma_\varepsilon = 1.3$ is the Prandtl number of k equation and ε equation respectively; the value of S_k , S_ε , $Y_M = 0$.

The velocity of turbulent flow is determined by the following formula:

$$\mu_\varepsilon = \rho C_\mu \frac{k^2}{\varepsilon} \quad (7)$$

where, C_μ is a constant, in the experiment $C_\mu = 0.09$.

Grid division and discrete method: The physical model of the nozzle is modeling using Solidworks

software, with ICEM CFD carrying on the grid division and finally using CFX for nozzle's internal flow field simulation. The low Re number of $k-\epsilon$ model is used to solve the problem of the flow in the near wall of the nozzle. The SIMPLE algorithm, which is based on the finite volume method and unstructured mesh, was used to realize the discretization of the nozzle structure.

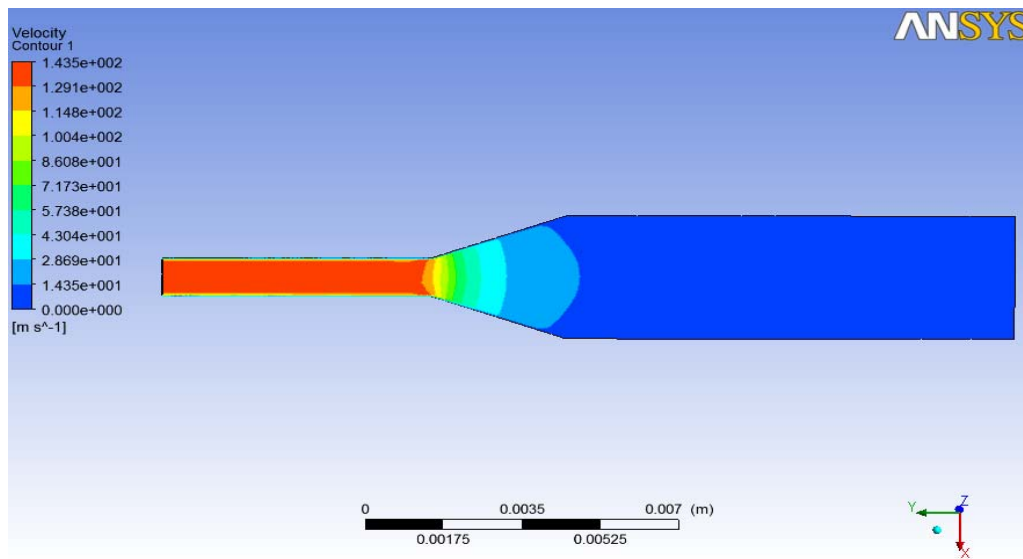
The standard model of turbulence model is selected and the internal flow field of the nozzle is single phase flow. Some factors such as phase change, heat transfer and so on are neglected in the model. The boundary conditions as follows: The jet inlet velocity is $v = Q/A$, of which $Q = 60$ L/min. The relative static pressure of jet flow is zero. Around the jet and its

export medium is water, at 20°C under the density of 1000 kg/m^3 , kinematic viscosity is $\nu = 1.003 \times 10^{-6} \text{ m}^2/\text{s}$.

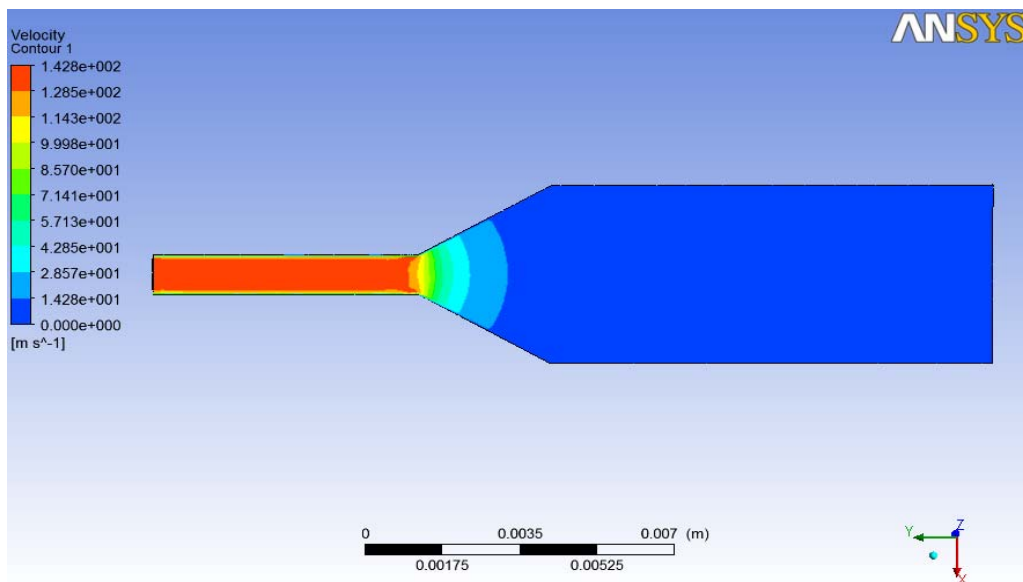
RESULTS AND DISCUSSION FOR NUMERICAL SIMULATION ANALYSIS WITH CFX

The influence of contraction angle ϕ on velocity: The velocity contours of 40-100° of contraction angle are shown in Fig. 3.

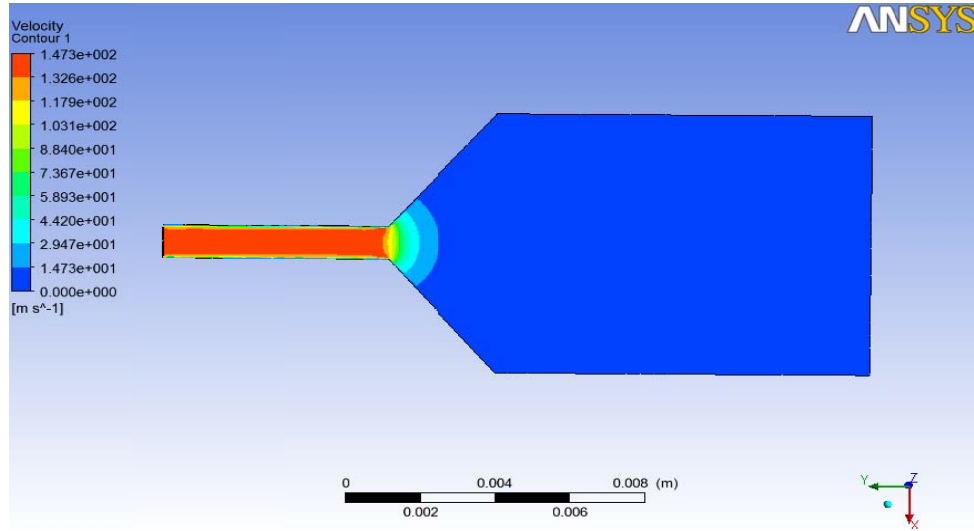
It can be seen from the Fig. 3 that the velocity in the interior of the nozzle is significantly changed in the contraction section and the outlet section. In the nozzle, the velocity contours are symmetrically distributed and the closer to the nozzle exit, the higher the velocity value is. The velocity distribution at the outlet of the



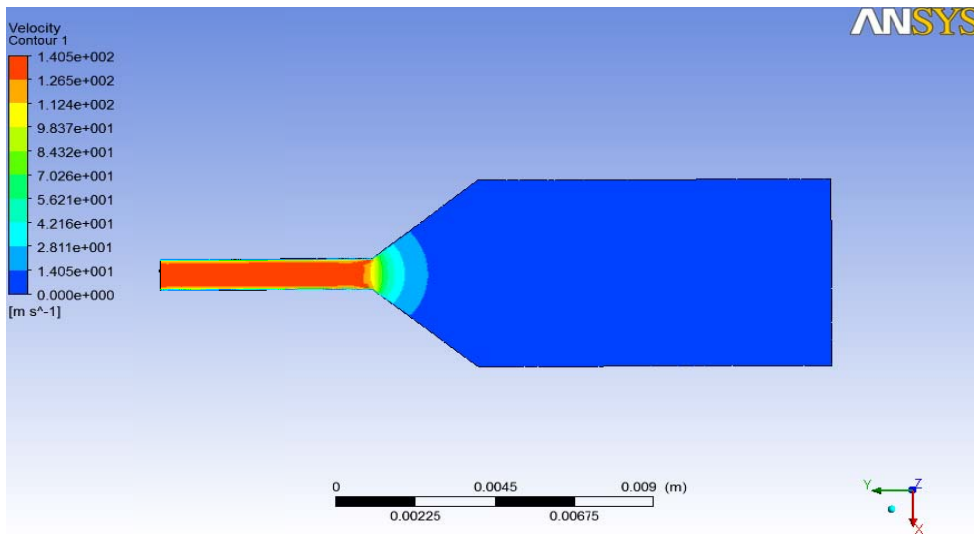
(a)



(b)



(c)



(d)

Fig. 3: The velocity contours of 40-100° of contraction angle; (a): $\varphi = 40^\circ$; (b): $\varphi = 60^\circ$; (c): $\varphi = 80^\circ$; (d): $\varphi = 100^\circ$



(a)

(b)

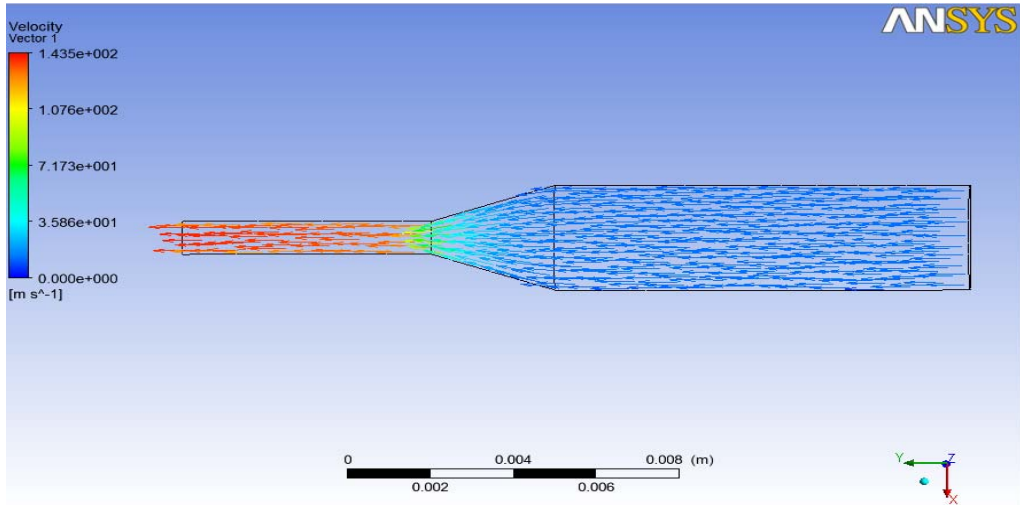
Fig. 4: Blast injury of scallop adductor muscle; (a): $\varphi < 60^\circ$; (b): $\varphi \geq 60^\circ$

nozzle decreases with the increase of the cone angle of the nozzle. When the nozzle cone angle is 60° , the outlet velocity curve in the range of 0.1 to 0.9 is almost a straight line, namely in the outlet diameter of 80% of the range, cone angle is 60° of nozzle jet for uniform distribution.

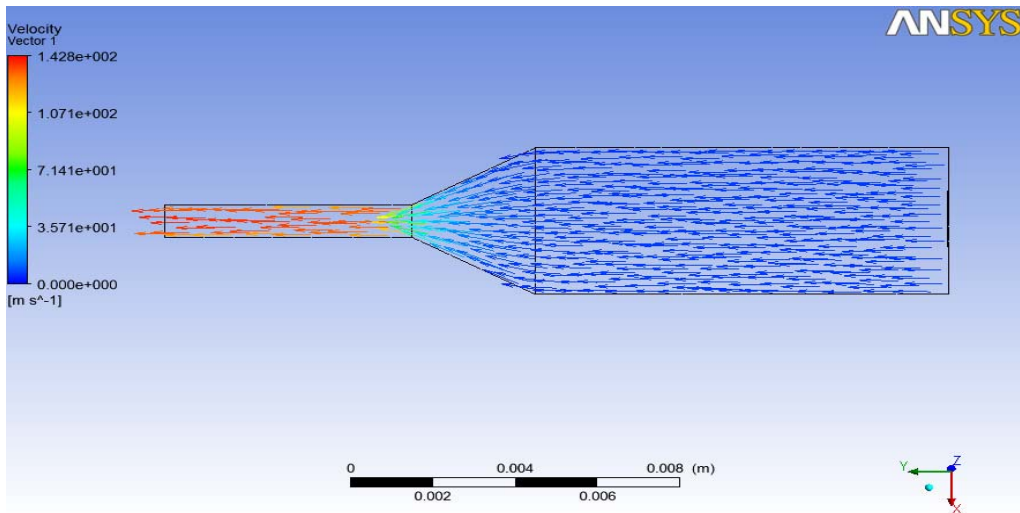
When the nozzle cone angle is less than 60° , the nozzle exit velocity reached 42.1 m/s (Fig. 3). But at this speed, the scallop adductor muscle surface has obvious wound because of water jet impact (Fig. 4).

When the cone angle is more than 100° , the larger cone angle, the larger diameter nozzle entrance and so the inlet velocity of the nozzle is greatly reduced. Shucking processing cannot be carried out normally at low speed. Therefore, it can be concluded that the cone angle of the narrow angle sector is the best when the cone angle $\varphi = 60^\circ$.

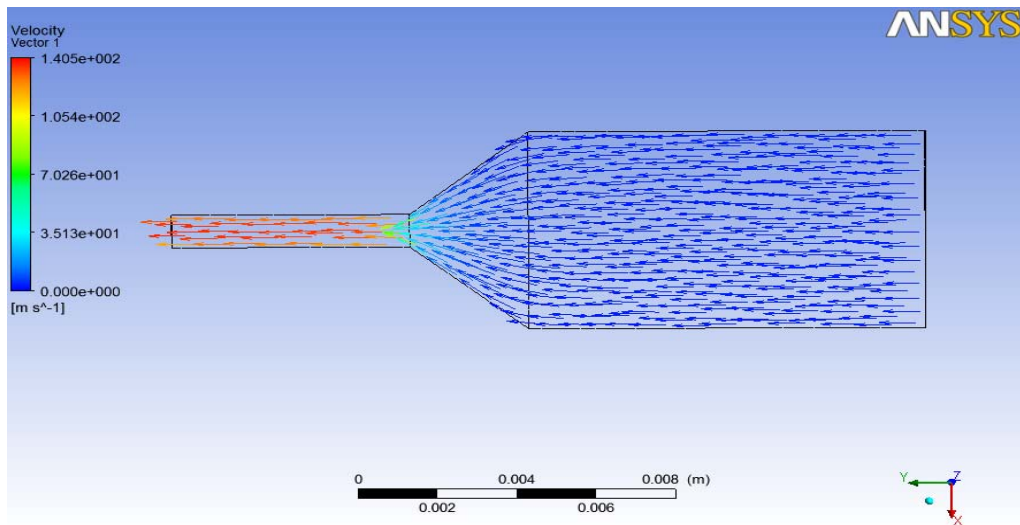
Figure 5 is the velocity vector diagram of 40°-100° of contraction angle. It can be seen from Fig. 5. The contraction angle determines whether there is internal flow of vortex appeared. The existence of vortex has a significant influence on the jet velocity distribution at



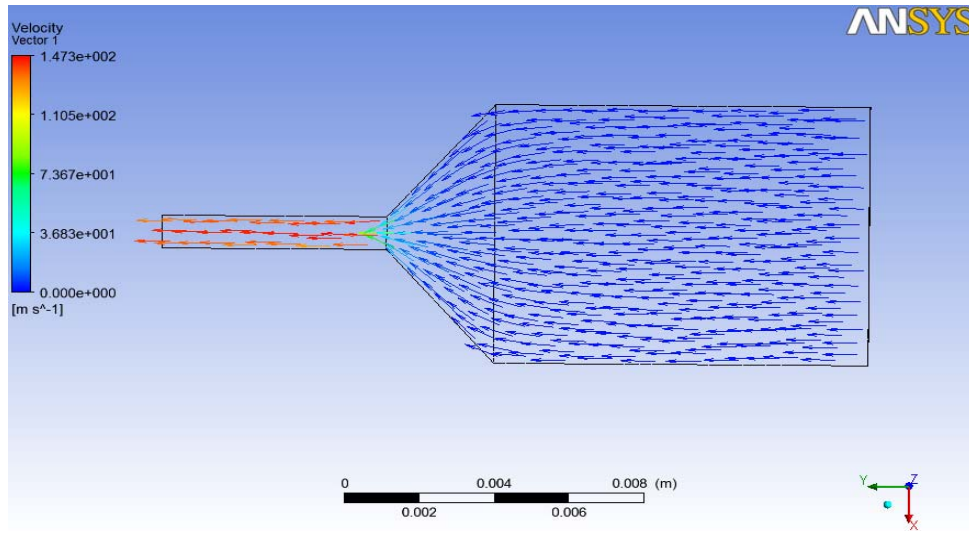
(a)



(b)



(c)



(d)

Fig. 5: The velocity vector diagram of 40-100° of contraction angle φ ; (a): $\varphi = 40^\circ$; (b): $\varphi = 60^\circ$; (c): $\varphi = 80^\circ$; (d): $\varphi = 100^\circ$

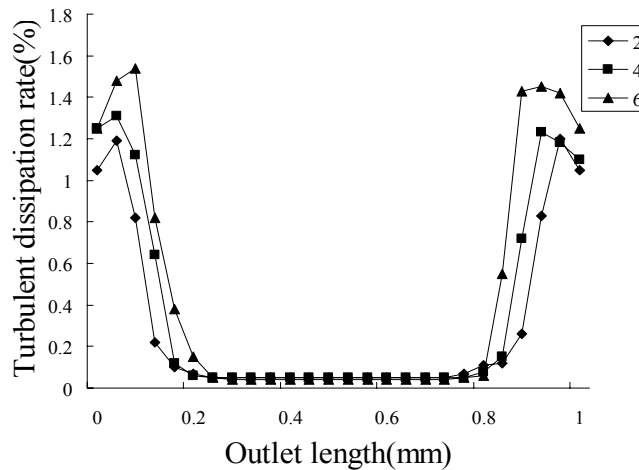


Fig. 6: Turbulent dissipation rate at different outlet length L

the nozzle exit, the flow in the nozzle and the loss of the nozzle. Under the condition of 100° , the vortex is more serious. With the decrease of the contraction angle, the vortex gradually disappeared. The velocity at the exit will become more and more uniform with the decrease of the vortex, the flow of the jet in the nozzle will become better and the corresponding nozzle loss will be reduced. Simulation results show that the acceleration of the flow is more stable at $\varphi = 60^\circ$.

In summary, the most suitable cone angle for the nozzle is $\varphi = 60^\circ$.

The influence of outlet length s on velocity: The turbulent dissipation rate distribution at the outlet is shown in Fig. 6.

Figure 6 reflects the change of the turbulent dissipation rate at the exit of the outlet. The dissipation

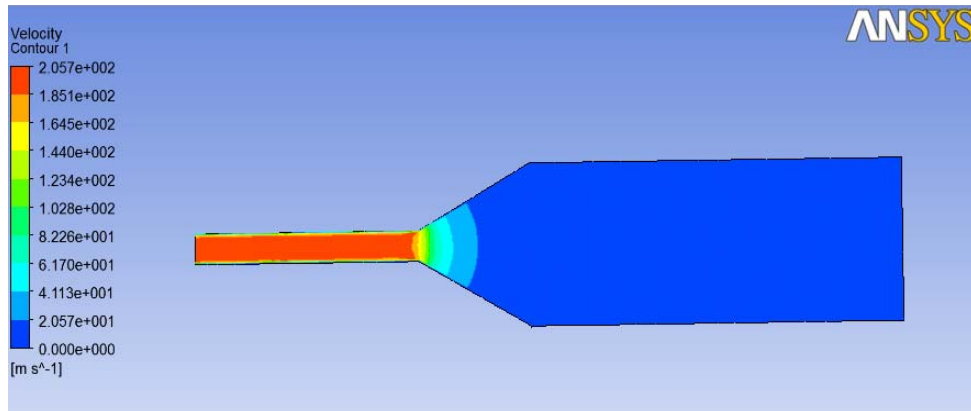
rate at the outlet is stable and its value is about 0.03. However, the turbulence intensity at the inner wall of the nozzle is changed rapidly and the turbulent dissipation rate is increased to 1.15. The turbulent dissipation rate indicates the amount of energy is lost. The greater the dissipation rate, the greater the energy loss. At the same time, the outlet length is neither too large nor too short, too long will increase the processing difficulty and lead to increased cost and too short will reduce the strength of the nozzle exit and shorten the service life of the nozzle. Therefore, the outlet length of the narrow angle sector nozzle $L = 4$ mm is suitable.

The influence of outlet diameter d on velocity: The changes of the length of the export nozzle internal flow velocity contour are shown in Fig. 7. Where, $\varphi = 60^\circ$, inlet diameter $D = 4.46$ mm and outlet diameter $d = 0.8-1.2$ mm.

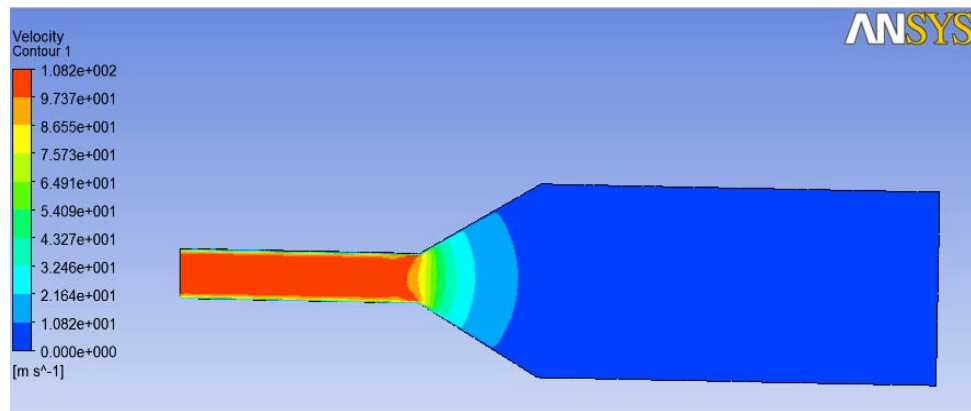
In Fig. 7, when the outlet diameter of the narrow angle sector nozzle is $d = 0.8$ mm, the velocity field of the outlet is not uniform and the high speed area appears. And the smaller the outlet diameter, the higher the processing difficulty, the nozzle processing costs also increased accordingly. When the nozzle diameter is $d = 1$ mm, the distribution of velocity field is uniform.

When the outlet diameter is $d = 1.2$ mm, the velocity field of the outlet velocity field is not uniform.

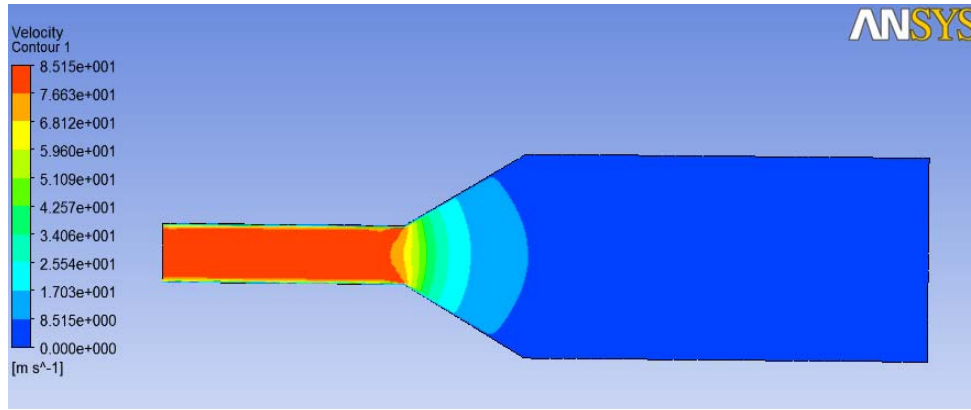
Figure 8 shows the turbulent energy dissipation rate of different outlet diameters. According to this figure, the smaller the outlet diameter, the greater the turbulence dissipation rate on the inner wall of the nozzle, that is, the greater the energy loss. When the



(a)



(b)



(c)

Fig. 7: Nozzle velocity flow field at different d ; (a): $d = 0.8$ mm; (b): $d = 1.0$ mm; (c): $d = 1.2$ mm

Table 1: The optimal configuration of nozzle

Parameter name	D	d	ϕ	S
Values	4.46 mm	1 mm	60°	4 mm

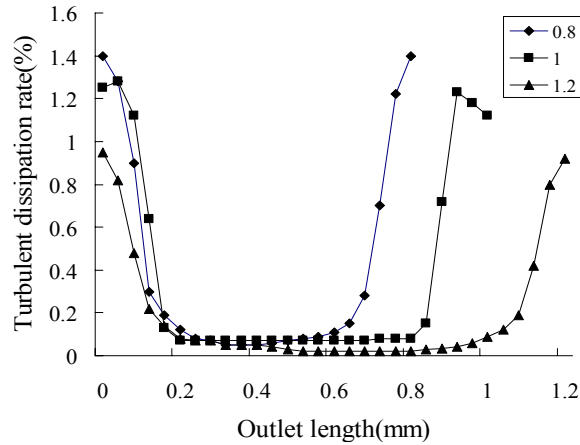


Fig. 8: Turbulent dissipation rate at different outlet diameter d

outlet diameter of the nozzle is $d = 1.2$ mm, the dissipation rate is lower, but the outlet flow rate is lower. When $d = 1$ mm, the velocity field is uniform, without the high velocity zone.

From the analysis of Fig. 7 and 8, it can be concluded that the outlet diameter $d = 1$ mm is more suitable.

The simulation results show that the nozzle parameters on the velocity distribution were further optimized contrast with previously published work (Qiushi, 2014; Xie, 2015) and the test results show that the simulation results are correct.

CONCLUSION

Using the CFX software, the internal flow field of the narrow angle sector nozzle was simulated by the standard k- ϵ turbulence model and the influence of the nozzle parameters on the velocity distribution was analyzed:

- The effect of cone angle ϕ on the flow velocity of nozzle outlet is larger and the smaller the cone angle ϕ , the higher the outlet flow velocity is. The cone angle of nozzle is optimized to find the suitable angle $\phi = 60^\circ$ for scallop processing;
- The length of outlet L has a little effect on the flow velocity of the jet flow. But for the energy loss and nozzle service life, the length of outlet $L = 4$ mm is the most suitable;
- Influence of outlet diameter d of jet velocity is larger. When d is too small, the processing is difficult with high processing costs; when d is too large, it will reduce the jet velocity at the outlet, not suitable for scallop processing. Test results show that outlet diameter $d = 1$ mm is the most suitable;

- In summary, the change of nozzle parameters will affect the injection performance, so the reasonable configuration of the nozzle parameters is very important. Test results show that the optimal configuration of the narrow angle sector nozzle is shown in Table 1.

ACKNOWLEDGMENT

The authors thank Science and Technology Project of China National Marine Public Welfare Industry "(201205031) and Science and Technology Support Program of Hebei Province (10221013, 12271008D) for support.

REFERENCES

- Cooper, L., 2010. Scallop Shucking and Handling Practices. 2nd Edn., Food Standards Agency, Scotland.
- Cruz-Romero, M., M. Smiddy, C. Hill, J.P. Kerry and A.L. Kelly, 2004. Effects of high pressure treatment on physicochemical characteristics of fresh oysters (*Crassostrea gigas*). Innov. Food Sci. Emerg., 5(2): 161-169.
- Cuili, H. and L. Sai, 2001. Physiological active substance and medicinal value of scallop. Chinese J. Mar. Drug., 20(02): 45-47.
- Currie, I.G., 2012. Fundamental Mechanics of Fluids. 4th Edn., CRC Press, Lincoln, NE, U.S.A.
- Dunn, P.G., T.G.H. Meyer and M. Hood, 2000. Advances in surface preparation, jet machining and food processing. Proceeding of the 6th Pacific Rim International Conference on Water Jet Technology. Centre for Mining Technology and Equipment (CMTE), Oct. 9-11, pp: 11-18.

- He, H., R.M. Adams, D.F. Farkas and M.T. Morrissey, 2002. Use of high-pressure processing for oyster shucking and shelf-life extension. *J. Food Sci.*, 67(2): 640-645.
- Hreha, P., S. Hloch, D. Magurová, J. Valíček, D. Kozak, M. Harnicarova and M.B. Rakin, 2010. Water jet technology used in medicine. *Tehnicki Vjesnik*, 17(2): 237-240.
- Li, Q.S., J.Z. Wang, J.G. Yi and H.Y. Jiang, 2013. Development state and prospect of bay scallop's adductor splitting service. *Guangdong Agr. Sci.*, 10: 198-201.
- Li, W.Q., J. Wang, J.F. Sun and W.S. Li, 2011. The nutrients analysis and evaluation of argopectens irradias. *Acta Nutr. Sin.*, 33(6): 630-632.
- Lunn, J. and H.E. Theobald, 2006. The health effects of dietary unsaturated fatty acids. *Nutr. Bull.*, 31(3): 178-224.
- Martin, D.E., 2004. Optimization and automation of a thermal oyster shucking process. LSUPLD Thesis, UMI Company, Ann Arbor.
- Martin, D.E. and S.G. Hall, 2006. Oyster shucking technologies: Past and present. *Int. J. Food Sci. Tech.*, 41(3): 223-232.
- Namba, K., M. Kobayashi, S. Aida, K. Uematsu, M. Yoshida, Y. Kondo and Y. Miyata, 1995. Persistent relaxation of the adductor muscle of oyster *Crassostrea gigas* induced by magnesium ion. *Fish. Sci.*, 61(2): 241-244.
- Papachristou, D.N. and R. Barters, 1982. Resection of the liver with a water jet. *Brit. J. Surg.*, 69(2): 93-94.
- Qiushi, L., 2014. The mechanism and experimental study of adductor muscle shucking based on water jet. M.S. Thesis, Agriculture University of Hebei, Baoding, Hebei Province.
- Xie, Q.Y., 2015. Experimental research and prototype design of water jet stripping bay scallop adductor muscle. M.S. Thesis, Agriculture University of Hebei, Baoding, Hebei Province.
- Yoshiaki, T., 2006. Water jet technology for medicine and biology. *JSAT*, 50(5): 257-260.